

# 4*f*-derived Fermi Surfaces of CeRu<sub>2</sub>(Si<sub>1-x</sub>Ge<sub>x</sub>)<sub>2</sub> near the Quantum Critical Point: Resonant Soft X-ray ARPES Study

T. Okane,<sup>1,\*</sup> T. Ohkochi,<sup>1</sup> Y. Takeda,<sup>1</sup> S.-i. Fujimori,<sup>1</sup> A. Yasui,<sup>1</sup> Y. Saitoh,<sup>1</sup> H. Yamagami,<sup>1,2</sup>  
A. Fujimori,<sup>1,3</sup> Y. Matsumoto,<sup>4</sup> M. Sugi,<sup>4</sup> N. Kimura,<sup>4</sup> T. Komatsubara,<sup>4</sup> and H. Aoki<sup>4</sup>

<sup>1</sup> *Synchrotron Radiation Research Center, Japan Atomic Energy Agency, Hyogo 679-5148, Japan*

<sup>2</sup> *Department of Physics, Kyoto Sangyo University, Kyoto 603-8555, Japan*

<sup>3</sup> *Department of Physics, University of Tokyo, Tokyo 113-0033, Japan*

<sup>4</sup> *Graduate School of Science and Center for Low Temperature Science, Tohoku University, Miyagi 980-8577, Japan*

(Dated: July 14, 2021)

Angle-resolved photoelectron spectroscopy in the Ce 3*d*→4*f* excitation region was measured for the paramagnetic state of CeRu<sub>2</sub>Si<sub>2</sub>, CeRu<sub>2</sub>(Si<sub>0.82</sub>Ge<sub>0.18</sub>)<sub>2</sub>, and LaRu<sub>2</sub>Si<sub>2</sub> to investigate the changes of the 4*f* electron Fermi surfaces around the quantum critical point. While the difference of the Fermi surfaces between CeRu<sub>2</sub>Si<sub>2</sub> and LaRu<sub>2</sub>Si<sub>2</sub> was experimentally confirmed, a strong 4*f*-electron character was observed in the band structures and the Fermi surfaces of CeRu<sub>2</sub>Si<sub>2</sub> and CeRu<sub>2</sub>(Si<sub>0.82</sub>Ge<sub>0.18</sub>)<sub>2</sub>, consequently indicating a delocalized nature of the 4*f* electrons in both compounds. The absence of Fermi surface reconstruction across the critical composition suggests that SDW quantum criticality is more appropriate than local quantum criticality in CeRu<sub>2</sub>(Si<sub>1-x</sub>Ge<sub>x</sub>)<sub>2</sub>.

PACS numbers: 71.18.+y, 71.27.+a, 75.30.Kz, 79.60.-i

Heavy-Fermion (HF) metals have attracted much attention in recent years as a prototypical system to study quantum criticality [1]. In rare-earth-based HF metals, e.g., Ce compounds, the ground state is considered to change from nonmagnetic to magnetic state at a boundary called quantum critical point (QCP) as a function of the relative strengths of Ruderman-Kittel-Kasuya-Yosida (RKKY) interaction to Kondo effect, and at the same time the Ce 4*f* electrons are transformed from itinerant to localized ones. CeRu<sub>2</sub>(Si<sub>1-x</sub>Ge<sub>x</sub>)<sub>2</sub> is an ideal system to study this QCP phenomena. CeRu<sub>2</sub>Si<sub>2</sub> is a representative HF compound with a paramagnetic ground state, exhibiting a metamagnetic transition at a magnetic field of  $H_m = 7.7$  T. The large specific heat coefficient  $\gamma \sim 350$  mJ/mol K<sup>2</sup> [2] indicates the itinerancy of the Ce 4*f* electrons in the ground state, and the Kondo crossover temperature  $T_0$  is estimated to be  $\sim 20$ -25 K [3, 4]. A magnetic ground state appears upon substitution of Ge atoms for Si atoms, corresponding to the application of a negative chemical pressure: The system is antiferromagnetic for  $x = 0.07$ -0.57, ferromagnetic for  $x = 0.57$ -1.0 [5, 6], and thus the critical composition  $x_c = 0.07$ .

If the 4*f* electrons of the nonmagnetic Ce compound like CeRu<sub>2</sub>Si<sub>2</sub> are itinerant and participate in the formation of Fermi surfaces (FSs), the total volume of the FSs should differ from that of the corresponding La compound, LaRu<sub>2</sub>Si<sub>2</sub>, owing to the contribution of one 4*f* electron per unit cell. This FS variation is accompanied by the variation of the band structures near the Fermi level ( $E_F$ ) through hybridization between the Ce 4*f* electrons and conduction electrons, i.e., the formation of *c-f* hybridized bands, and in this sense, one can say that the energy bands have a 4*f* electron character. According to band structure calculations on CeRu<sub>2</sub>Si<sub>2</sub> and LaRu<sub>2</sub>Si<sub>2</sub> [7], when the Ce 4*f* electrons of CeRu<sub>2</sub>Si<sub>2</sub> are assumed

to be itinerant, the formation of the *c-f* hybridized bands leads to the emergence of FS which includes a contribution from heavy 4*f* electrons. The de Haas van Alphen (dHvA) experiment for CeRu<sub>2</sub>Si<sub>2</sub> [8] indicated the existence of the heavy-electron FS branches, which would correspond to the above-mentioned 4*f*-originated FS. On the other hand, the dHvA experiments indicated that the FSs of ferromagnetic CeRu<sub>2</sub>Ge<sub>2</sub> are almost the same as those of LaRu<sub>2</sub>Ge<sub>2</sub>, indicating that the 4*f* electrons are localized in CeRu<sub>2</sub>Ge<sub>2</sub> [9, 10, 11]. Therefore, the Ce 4*f* electrons turn from itinerant to localized ones in going from CeRu<sub>2</sub>Si<sub>2</sub> to CeRu<sub>2</sub>Ge<sub>2</sub>, and the experimental determination whether the FSs of Ce-based compounds are the same or not as those of corresponding La compound is directly connected with the fact whether the Ce 4*f* electrons are itinerant or localized.

The purpose of this paper is an investigation of the FS variation around the QCP of CeRu<sub>2</sub>(Si<sub>1-x</sub>Ge<sub>x</sub>)<sub>2</sub> by soft X-ray angle-resolved photoelectron spectroscopy (ARPES). To avoid a magnetic reconstruction of FSs, the ARPES measurements were performed in the temperature range  $T_N < T \leq T_0$ . As a consequence, we have checked which of two scenarios for the quantum criticality of the HF metals is appropriate; the spin-density-wave (SDW) QCP model or the local quantum criticality (LQC) model. As illustrated in a schematic diagram in Fig. 1, a FS crossover is expected just around the QCP in the LQC model, while it is unnecessary in the SDW-QCP model [1, 12, 13]. It is still controversial which scenario is appropriate in the HF metals [14, 15, 16, 17, 18, 19, 20], and the direct observation of the FS reconstruction at the QCP has never been successful. ARPES experiments were previously performed to investigate the FSs of CeRu<sub>2</sub>Si<sub>2</sub> and its related compounds in the VUV (20-200 eV) [21] and the soft X-ray (700-860 eV) regions [22].

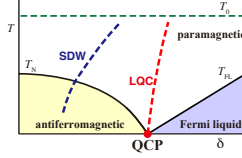


FIG. 1: (color online) Schematic phase diagram for QCP of HF metal [1]. It is illustrated against temperature versus control parameter  $\delta$  which represents the strength ratio of Kondo effect to RKKY interaction.  $T_N$ ,  $T_{FL}$ , and  $T_0$  designate the Néel temperature, the onset temperature of Fermi liquid behavior, and the crossover temperature where Kondo screening sets in, respectively. Blue and red broken lines represent a crossover from the  $4f$ -delocalized FSs to the  $4f$ -localized FSs in the SDW-QCP model and the LQC model, respectively.

While Denlinger *et al.* [21] could not observe a clear difference of FSs between  $\text{CeRu}_2\text{Si}_2$  and  $\text{LaRu}_2\text{Si}_2$ , Yano *et al.* [22] claimed the observation of  $4f$ -delocalized FSs for  $\text{CeRu}_2\text{Si}_2$  and  $4f$ -localized FSs for  $\text{CeRu}_2\text{Ge}_2$  even in the paramagnetic state. Therefore, it is expected that soft X-ray ARPES experiments for  $\text{CeRu}_2(\text{Si}_{1-x}\text{Ge}_x)_2$  can verify the existence of the FS crossover around the QCP of this system. In order to enhance the photoemission signals of the Ce  $4f$  electrons, we have performed ARPES experiment in the Ce  $3d \rightarrow 4f$  resonance energy region and successfully observed the strongly  $c$ - $f$  hybridized FS both for  $\text{CeRu}_2\text{Si}_2$  and  $\text{CeRu}_2(\text{Si}_{0.82}\text{Ge}_{0.18})_2$ , below and above  $x_c = 0.07$ , respectively. ARPES was also measured for  $\text{LaRu}_2\text{Si}_2$  as a reference material where the  $4f$  electrons do not participate in the FS formation.

All the measured samples were single crystals grown in the procedures described in Ref. 6. ARPES measurements were performed at beamline BL23SU of SPring-8. The energy resolution was 120 meV for  $\text{CeRu}_2\text{Si}_2$  and 160 meV for  $\text{CeRu}_2(\text{Si}_{0.82}\text{Ge}_{0.18})_2$  at  $h\nu = 881$  eV, and 170 meV at  $h\nu = 770$ -870 eV. Clean sample surfaces were obtained by *in situ* cleaving along [001] surface. The sample temperature was 20 K, comparable to  $T_0$  of  $\text{CeRu}_2\text{Si}_2$

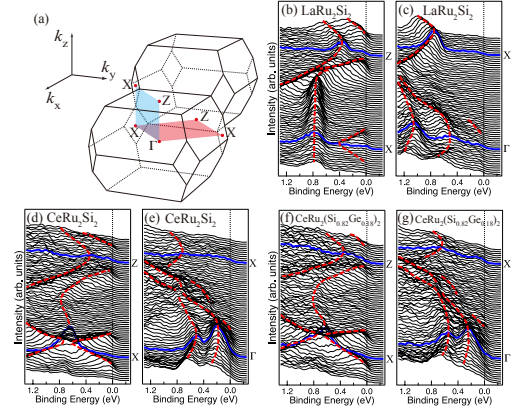


FIG. 2: (color online) (a) Brillouine zone (BZ) for  $\text{CeRu}_2(\text{Si}_{1-x}\text{Ge}_x)_2$ . Red and blue planes signify the measured plane by the angle-scanning and the  $h\nu$ -scanning measurements, respectively. Off-resonance ARPES spectra of  $\text{LaRu}_2\text{Si}_2$  along the X-Z (b) and  $\Gamma$ -X (c) directions, those of  $\text{CeRu}_2\text{Si}_2$  along the X-Z (d) and  $\Gamma$ -X (e) directions, and those of  $\text{CeRu}_2(\text{Si}_{0.82}\text{Ge}_{0.18})_2$  along the X-Z (f) and  $\Gamma$ -X (g) directions. Red broken lines indicate dispersive energy bands.

and above  $T_N \sim 8$  K of  $\text{CeRu}_2(\text{Si}_{0.82}\text{Ge}_{0.18})_2$ .

Figures 2(b) and 2(c), 2(d) and 2(e), 2(f) and 2(g) show ARPES spectra of the valence bands of  $\text{LaRu}_2\text{Si}_2$ ,  $\text{CeRu}_2\text{Si}_2$ , and  $\text{CeRu}_2(\text{Si}_{0.82}\text{Ge}_{0.18})_2$ , respectively, along the X-Z and  $\Gamma$ -X directions of the Brillouine zone (BZ) illustrated in Fig. 2(a), obtained from the angle-scanning measurements. The angle-scanning measurements were performed at photon energies  $h\nu$  corresponding to the  $\Gamma$ -X-Z plane, i.e.,  $h\nu = 765, 860$ , and  $855$  eV for  $\text{LaRu}_2\text{Si}_2$ ,  $\text{CeRu}_2\text{Si}_2$ , and  $\text{CeRu}_2(\text{Si}_{0.82}\text{Ge}_{0.18})_2$ , respectively, which were chosen by assuming the inner potential value of 12 eV [21, 22]. These cases are called *off-resonance* hereafter. As indicated by the red broken lines, the observed dispersions of energy bands are quite similar between  $\text{CeRu}_2\text{Si}_2$  and  $\text{CeRu}_2(\text{Si}_{0.82}\text{Ge}_{0.18})_2$ . On the other hand, the energy dispersions of  $\text{LaRu}_2\text{Si}_2$  are remarkably different from those of  $\text{CeRu}_2\text{Si}_2$ : For example, the energy positions of the band structures at the  $\Gamma$  point are located on the higher binding energy side in  $\text{LaRu}_2\text{Si}_2$  than in  $\text{CeRu}_2\text{Si}_2$ . The difference originates from the participa-

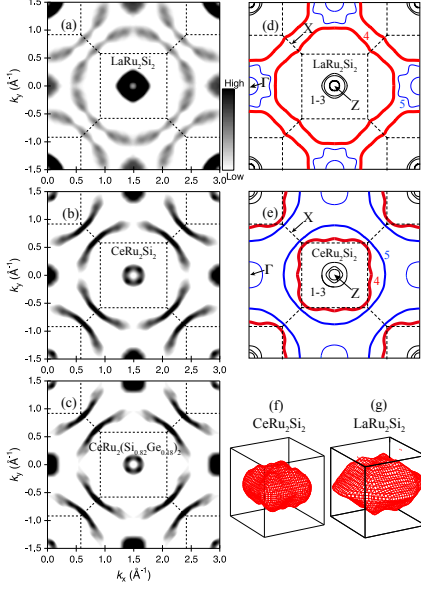


FIG. 3: (color online) Off-resonance FS images of  $\text{LaRu}_2\text{Si}_2$  (a),  $\text{CeRu}_2\text{Si}_2$  (b), and  $\text{CeRu}_2(\text{Si}_{0.82}\text{Ge}_{0.18})_2$  (c) in the  $k_x$ - $k_y$  plane, compared with calculated FSs of  $\text{LaRu}_2\text{Si}_2$  (d) and  $\text{CeRu}_2\text{Si}_2$  (e) [7]. In (d) and (e), numbers designate the label of each FS, the same as used in Refs. 21 and 22, and red and blue lines represent the hole FS of band 4 and the electron FS of band 5, respectively. BZ is illustrated by broken lines. Calculated 3D images of the hole FS of band 4 of  $\text{CeRu}_2\text{Si}_2$  (f) and  $\text{LaRu}_2\text{Si}_2$  (g) around the Z point (body center) [7].

tion of the Ce 4*f* electrons in the energy band formation, and thus it suggests the delocalized nature of the 4*f* electrons both in  $\text{CeRu}_2\text{Si}_2$  and  $\text{CeRu}_2(\text{Si}_{0.82}\text{Ge}_{0.18})_2$ .

Figures 3(a)-3(c) display off-resonance FS images of  $\text{LaRu}_2\text{Si}_2$ ,  $\text{CeRu}_2\text{Si}_2$ , and  $\text{CeRu}_2(\text{Si}_{0.82}\text{Ge}_{0.18})_2$ , respectively, represented by the intensities of the ARPES spectra integrated near Fermi energy ( $E_F$ ) as a function of momenta ( $k_x, k_y$ ). For comparison, the calculated FSs of  $\text{LaRu}_2\text{Si}_2$  and  $\text{CeRu}_2\text{Si}_2$  in the  $k_x$ - $k_y$  plane [7] are shown in Figs. 3(d) and 3(e), respectively. The numbers 1-4 and 5 designate the hole FSs and the electron FS, respectively. Figures 3(f) and 3(g) show the calculated three-dimensional (3D) images of the large hole FS of band 4 of  $\text{CeRu}_2\text{Si}_2$  and  $\text{LaRu}_2\text{Si}_2$ , respectively, indicating a significant volume variation due to participation of the Ce 4*f* electrons in the FS formation [7]. A large FS surrounding the Z point was experimentally detected in every compound. While the experimental

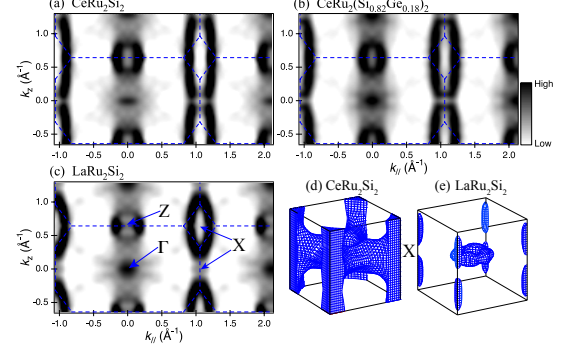


FIG. 4: (color online) FS images of  $\text{CeRu}_2\text{Si}_2$  (a),  $\text{CeRu}_2(\text{Si}_{0.82}\text{Ge}_{0.18})_2$  (b), and  $\text{LaRu}_2\text{Si}_2$  (c) in the  $k_{xy}$ - $k_z$  plane. BZ is indicated by blue broken lines. Calculated 3D images of the electron FS of band 5 of  $\text{CeRu}_2\text{Si}_2$  (d) and  $\text{LaRu}_2\text{Si}_2$  (e) around the  $\Gamma$  point (body center) [7].

large FS of  $\text{LaRu}_2\text{Si}_2$  has a square shape and agrees well with the calculated hole FS of band 4, the experimental large FS of  $\text{CeRu}_2\text{Si}_2$  has a circular shape and agrees well with the calculated electron FS of band 5. The large FS of  $\text{CeRu}_2(\text{Si}_{0.82}\text{Ge}_{0.18})_2$  is almost identical to that of  $\text{CeRu}_2\text{Si}_2$ . However, the above assignment for the Ce compounds is not conclusive because the hole FS of band 4 shown in Fig. 3(e) is not observed both in  $\text{CeRu}_2\text{Si}_2$  and  $\text{CeRu}_2(\text{Si}_{0.82}\text{Ge}_{0.18})_2$ . Because the hole FS of band 4 is considered to be the heaviest FS branch due to the largest contribution of the Ce 4*f* electrons [7, 8], the absence of this FS branch may deny the delocalized nature of the Ce 4*f* electrons.

Figures 4(a)-4(c) show FS images in the  $k_{xy}$ - $k_z$  plane of  $\text{CeRu}_2\text{Si}_2$ ,  $\text{CeRu}_2(\text{Si}_{0.82}\text{Ge}_{0.18})_2$ , and  $\text{LaRu}_2\text{Si}_2$ , respectively, obtained from the  $h\nu$ -scanning ARPES measurements (750-870 eV). The calculated 3D images of the electron FS of band 5 of  $\text{CeRu}_2\text{Si}_2$  and  $\text{LaRu}_2\text{Si}_2$  are shown in Figs. 4(d) and 4(e), respectively [7]. A noticeable difference between  $\text{CeRu}_2\text{Si}_2$  and  $\text{LaRu}_2\text{Si}_2$  is seen in the FS along the vertical X-X line; it has a connected tube-like shape in  $\text{CeRu}_2\text{Si}_2$ , while it has a closed ellip-

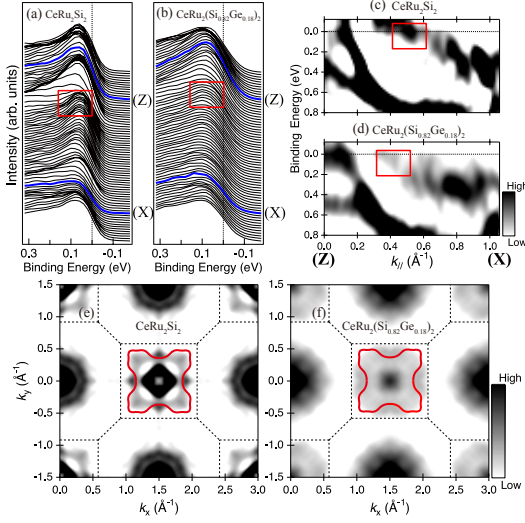


FIG. 5: (color online) On-resonance ARPES spectra of  $\text{CeRu}_2\text{Si}_2$  (a) and  $\text{CeRu}_2(\text{Si}_{0.82}\text{Ge}_{0.18})_2$  (b) along the line corresponding to the X-Z direction. Images of the band dispersion near  $E_F$  obtained from the on-resonance ARPES spectra of  $\text{CeRu}_2\text{Si}_2$  (c) and  $\text{CeRu}_2(\text{Si}_{0.82}\text{Ge}_{0.18})_2$  (d). Red squares in (a)-(d) signify the  $E_F$ -crossing point of the strongly  $c$ - $f$  hybridized bands. On-resonance FS images in the  $k_x$ - $k_y$  plane of  $\text{CeRu}_2\text{Si}_2$  (e) and  $\text{CeRu}_2(\text{Si}_{0.82}\text{Ge}_{0.18})_2$  (f), compared with the calculated hole FS of band 4 at  $k_z = 0.3\pi/c$  away from the  $\Gamma$ -Z-X plane, represented by red lines [7].

soidal shape in  $\text{LaRu}_2\text{Si}_2$ . The observed difference coincides with the difference in the calculated FS between Figs. 4(d) and 4(e) [7]. Therefore, this difference gives a good criterion whether the Ce  $4f$  electrons participate in the FS formation, and the present result have confirmed that the FSs of  $\text{CeRu}_2\text{Si}_2$  are obviously different from the FSs of  $\text{LaRu}_2\text{Si}_2$ . The FS of  $\text{CeRu}_2(\text{Si}_{0.82}\text{Ge}_{0.18})_2$  along the X-X line has a tube-like shape as in  $\text{CeRu}_2\text{Si}_2$ , indicating that the  $4f$  electrons contribute to the energy-band formation in  $\text{CeRu}_2(\text{Si}_{0.82}\text{Ge}_{0.18})_2$ . A remaining problem is that the difference between  $\text{CeRu}_2\text{Si}_2$  and  $\text{LaRu}_2\text{Si}_2$ , which the large FS surrounding Z point should be composed of bands 4 and 5 in  $\text{CeRu}_2\text{Si}_2$  and only of band 4 in  $\text{LaRu}_2\text{Si}_2$ , is not clearly observed.

The reason why the strongly  $c$ - $f$  hybridized hole FS is not observed in the off-resonance ARPES might be that the observed FS originate from the bands of

major contribution from Ru  $4d$  electrons. Therefore, angle-scanning measurements were performed at the Ce  $3d \rightarrow 4f$  resonant energy of  $h\nu = 881\text{eV}$  for  $\text{CeRu}_2\text{Si}_2$  and  $\text{CeRu}_2(\text{Si}_{0.82}\text{Ge}_{0.18})_2$  to enhance the signals of the  $4f$  electrons. This case is called *on-resonance* hereafter. The resonance energy corresponds to  $k_z = 0.29\pi/c$  and  $0.37\pi/c$  for  $\text{CeRu}_2\text{Si}_2$  and  $\text{CeRu}_2(\text{Si}_{0.82}\text{Ge}_{0.18})_2$ , respectively. Figures 5(a) and 5(b) show on-resonance ARPES spectra of  $\text{CeRu}_2\text{Si}_2$  and  $\text{CeRu}_2(\text{Si}_{0.82}\text{Ge}_{0.18})_2$ , respectively. The spectral feature around  $0.1\text{eV}$ , which is remarkably enhanced in the on-resonance spectra, is peaky near the Z point but indistinct near the X point, indicating that the resonance enhancement is weak near the X point. In addition to the  $E_F$ -crossing bands which are the same as in the off-resonance spectra in Figs. 2(d) and 2(f), another  $E_F$ -crossing is observed as indicated by the red squares in Figs. 5(a) and 5(b). In order to make the dispersive bands near  $E_F$  clear, we have mapped images of secondary derivatives of the ARPES spectra where integrated intensities are normalized in momentum distribution curves, as shown in Figs. 5(c) and 5(d). One can see that additional bands, which are hardly discernible in the off-resonance spectra, cross  $E_F$  around the midpoint of the (X)-(Z) line, designated by red squares. Since the additional bands appear only in the on-resonance images, they are strongly  $c$ - $f$  hybridized bands. Figures 5(e) and 5(f) display on-resonance FS images of  $\text{CeRu}_2\text{Si}_2$  and  $\text{CeRu}_2(\text{Si}_{0.82}\text{Ge}_{0.18})_2$ , respectively. Surprisingly, the large circular FS surrounding the Z point in the off-resonance images becomes invisible in the on-resonance images. This might be due to the weakness of the resonance enhancement near the X point mentioned above. In addition, another FS appears just inside the square BZ boundary surrounding the Z point both in  $\text{CeRu}_2\text{Si}_2$  and  $\text{CeRu}_2(\text{Si}_{0.82}\text{Ge}_{0.18})_2$ . This FS corresponds to the  $E_F$ -crossing indicated by the red squares in Figs. 5(c) and 5(d). The size and shape of this FS are comparable to those of the calculated hole FS of band 4 at  $k_z = 0.3\pi/c$  away from the  $\Gamma$ -Z-X plane, shown by red lines in Figs. 5(e) and 5(f). Therefore, the FS observed only in the on-resonance images is attributed to the strongly  $c$ - $f$  hybridized heavy-quasi-particle FS.

The phase diagram in Fig. 1 indicates that, in the LQC model, the FS reconstruction is expected to occur when one crosses the critical composition  $x_c$  at a temperature well below  $T_0$ , even above  $T_N$ . The present result demonstrates that a discontinuous change of FS does not exist near the critical composition and the  $4f$ -delocalized FS regime is extended beyond the critical composition, although the measurements were performed at a temperature comparable to  $T_0$ . When the temperature is lowered from  $\sim T_0$  down to the temperature just above  $T_N$ , it is natural to think that the Ce  $4f$  electrons keep their itinerancy without a phase transition. Therefore, the absence of the FS change near the critical composition is strongly implied above  $T_N$ , and it can be claimed that

the SDW-QCP model is suitable for  $\text{CeRu}_2(\text{Si}_{1-x}\text{Ge}_x)_2$  rather than the LQC model.

In conclusion, we have shown that the Ce  $4f$  electrons in the paramagnetic state of  $\text{CeRu}_2(\text{Si}_{1-x}\text{Ge}_x)_2$  are itinerant and participate in the FS formation at both side of critical composition  $x_c = 0.07$ . The absence of the clear change of the FSs across the critical composition indicates that the SDW-QCP model is more likely than the LQC model in  $\text{CeRu}_2(\text{Si}_{1-x}\text{Ge}_x)_2$ . In future studies, the crossover below the magnetic-ordering temperature should be examined both at the paramagnetic-antiferromagnetic and antiferromagnetic-ferromagnetic boundaries of  $\text{CeRu}_2(\text{Si}_{1-x}\text{Ge}_x)_2$  by Ce  $3d \rightarrow 4f$  resonant ARPES.

We thank J. Otsuki for useful discussions. This work was performed under the Proposal No. 2008A3822 at SPring-8, supported by the Grant-in-Aid for Scientific Research on Innovative Areas of the MEXT, Japan.

---

\* Electronic address: okanet@spring8.or.jp

- [1] P. Gegenwart *et al.*, Nature Phys. **4**, 186 (2008).
- [2] M.J. Besnus *et al.*, Solid State Commun. **55**, 779 (1985).
- [3] A. Loidl *et al.*, Physica B. **156-157**, 794 (1989).
- [4] R.A. Fisher *et al.*, J. Low Temp. Phys. **84**, 49 (1991).
- [5] P. Haen *et al.*, Physica B. **259-261**, 85 (1999).
- [6] M. Sugi *et al.*, Phys. Rev. Lett. **101**, 056401 (2008).
- [7] H. Yamagami *et al.*, J. Phys. Soc. Jpn. **61**, 2388 (1992); J. Phys. Soc. Jpn. **62**, 592 (1993).
- [8] H. Aoki *et al.*, Phys. Rev. Lett. **71**, 2110 (1993).
- [9] C.A. King *et al.*, Physica B. **171**, 161 (1991).
- [10] H. Ikezawa *et al.*, Physica B. **237-238**, 210 (1997).
- [11] H. Yamagami *et al.*, J. Phys. Soc. Jpn. **63**, 2290 (1992).
- [12] Q. Si *et al.*, Nature **413**, 804 (2001).
- [13] Q. Si, Physica B **378-380**, 23 (2006).
- [14] R. K  chler *et al.*, Phys. Rev. Lett. **91**, 066405 (2003).
- [15] S. Paschen *et al.*, Nature **432**, 881 (2004).
- [16] A. Schr  der *et al.*, Nature **407**, 351 (2000).
- [17] R. K  chler *et al.*, Phys. Rev. Lett. **93**, 096402 (2004).
- [18] A.V. Silhanek *et al.*, Phys. Rev. Lett. **96**, 206401 (2006).
- [19] R. K  chler *et al.*, Phys. Rev. Lett. **96**, 256403 (2006).
- [20] H. Kadowaki *et al.*, Phys. Rev. Lett. **96**, 016401 (2006).
- [21] J.D. Denlinger *et al.*, J. Electron Spectrosc. Relat. Phenom. **117**, 347 (2001).
- [22] M. Yano *et al.*, Phys. Rev. Lett. **98**, 036405 (2007); Phys. Rev. B **77**, 035118 (2008).